

## Coulomb blockade thermometer: Tests and instrumentation

J. P. Kauppinen, K. T. Loberg, A. J. Manninen, J. P. Pekola, and R. A. Voutilainen

Citation: *Rev. Sci. Instrum.* **69**, 4166 (1998); doi: 10.1063/1.1149265

View online: <http://dx.doi.org/10.1063/1.1149265>

View Table of Contents: <http://rsi.aip.org/resource/1/RSINAK/v69/i12>

Published by the [American Institute of Physics](#).

---

### Related Articles

Note: Response characteristics of the sensor based on LaF3 thin film to different humidified gases  
*Rev. Sci. Instrum.* **83**, 056103 (2012)

Development of a simultaneous Hugoniot and temperature measurement for preheated-metal shock experiments: Melting temperatures of Ta at pressures of 100 GPa  
*Rev. Sci. Instrum.* **83**, 053902 (2012)

Development of a continuous testing apparatus for temperature reduction performance of cool coatings  
*Rev. Sci. Instrum.* **83**, 054901 (2012)

Transmission and temperature sensing characteristics of a selectively liquid-filled photonic-bandgap-fiber-based Sagnac interferometer  
*Appl. Phys. Lett.* **100**, 141104 (2012)

Communication: Hybrid femtosecond/picosecond rotational coherent anti-Stokes Raman scattering thermometry using a narrowband time-asymmetric probe pulse  
*J. Chem. Phys.* **136**, 111101 (2012)

---

### Additional information on *Rev. Sci. Instrum.*

Journal Homepage: <http://rsi.aip.org>

Journal Information: [http://rsi.aip.org/about/about\\_the\\_journal](http://rsi.aip.org/about/about_the_journal)

Top downloads: [http://rsi.aip.org/features/most\\_downloaded](http://rsi.aip.org/features/most_downloaded)

Information for Authors: <http://rsi.aip.org/authors>

## ADVERTISEMENT

### Precision Positioning Solutions

HEXAPODS, PIEZO STAGES & ACTUATORS



Hexapod 6-Axis Stages



Nanopositioning Stages



Piezo Actuators

**PI**

PI - leader in Piezo Mechanics  
Nanopositioning, Hexapods.

Standard, custom, vacuum,  
non-magnetic.

PI (Physik Instrumente) LP  
[www.pi-usa.us](http://www.pi-usa.us) 508.832.3456

## Coulomb blockade thermometer: Tests and instrumentation

J. P. Kauppinen,<sup>a)</sup> K. T. Loberg, A. J. Manninen, and J. P. Pekola

*Department of Physics, University of Jyväskylä, P.O. Box 35, FIN-40351 Jyväskylä, Finland and Nanoway Oy, Ylistönmäentie 31, FIN-40500 Jyväskylä, Finland*

R. A. Voutilainen

*RV-Elektroniikka Oy Picowatt, Veromiehentie 14, FIN-01510 Vantaa, Finland*

(Received 5 August 1998; accepted for publication 23 September 1998)

Coulomb blockade thermometry (CBT) provides a simple method for absolute thermometry in every day laboratory use at cryogenic temperatures. CBT has been found insensitive to even high magnetic fields. We review the principles and the operation of CBT and the fabrication of the sensors, and present new data on radiation hardness and stability of the sensors. We describe the instrumentation of CBT in detail. We have developed two signal conditioning units for CBT measurements. One is a modified alternating current resistance bridge, a versatile laboratory instrument operating with a PC computer, and the other one is a simple stand-alone instrument for direct temperature reading. Test results on their performance are also presented. Both prototypes have a short-term reproducibility of 0.3% or better in temperature measurement. © 1998 American Institute of Physics. [S0034-6748(98)03912-4]

### I. INTRODUCTION

#### A. Low temperature thermometry

Thermometers can be divided into two groups according to the level of knowledge about the physical basis of the underlying thermodynamic laws and quantities. For primary thermometers the measured property of matter is known so well that temperature can be calculated without any unknown quantities. Examples of these are thermometers based on the equation of state of a gas, on the velocity of sound in a gas, on the thermal noise voltage or current of an electrical resistor, and on the angular anisotropy of gamma ray emission of certain radioactive nuclei in a magnetic field. Primary thermometers are usually inconvenient and difficult to use.<sup>1,2</sup>

Secondary thermometers are most widely used because of their convenience. Also, they are often much more sensitive than primary ones. For secondary thermometers knowledge of the measured property is not sufficient to allow direct calculation of temperature. They have to be calibrated against a primary thermometer at least at one temperature or at a number of fixed temperatures. Such fixed points, for example, triple points and superconducting transitions, occur reproducibly at the same temperature. Examples of often used secondary thermometers are helium vapor pressure thermometer, <sup>3</sup>He melting pressure thermometer, thermometers based on thermoelectricity, dielectric-constant capacitive thermometers, magnetic thermometers with electronic or nuclear paramagnets, diode thermometers, and various resistors.<sup>1-3</sup>

Internationally agreed temperature scales are based on fixed points and interpolating thermometers. The most recent official temperature scale is ITS-90 from 1990.<sup>4</sup> It extends from 0.65 to above 1200 K. The fixed points of ITS-90 are

mostly phase transitions of pure materials. Presently, plans exist to extend the official scale to lower temperatures.<sup>5</sup>

Temperature  $T$  is one of the most important parameters in physics and technology and one of the basic quantities in all systems of units. This sets high requirements on a practical thermometer. One should be able to measure temperature with high *accuracy*. The thermometer should also maintain its accuracy in repeated thermal cycling as well as over a long period of time, that is, it should have high *reproducibility*. The signal that includes the temperature information must be *easily measured*. The thermometer should have high *sensitivity*  $(\Delta x/x)/(\Delta T/T)$  for the temperature parameter  $x$ , and high *resolution*, that is, even small temperature changes should be detectable. It is also recommended that the parameter  $x$  is at least *monotonic* and preferably *linear* in  $T$ . *Primarily* of the thermometer is profitable to avoid inconvenient and often expensive calibration. Magnetic fields are frequently present in cryogenic measurements and this should not decrease the reliability of temperature measurement. Therefore the thermometer should be *independent of magnetic field*. *Wide temperature range* is useful to make operation with only one thermometer or, at least, with one type of thermometer possible. To monitor or detect fast temperature changes, for example, in case of a quench of a superconducting magnet, requires fast *thermal* and *electronic response time* of the thermometer. This, in turn, requires small *heat capacity* and good *thermal contact* with the body whose temperature is to be measured, besides the electrical compatibility of the sensor in fast changes of  $T$ . Especially at very low temperatures, low *power dissipation* is important to avoid self heating. In some applications the thermometer should operate in harsh environments, like under *ionizing radiation* or in *ultrahigh vacuum*. *Robustness, ease of use, and low cost* are, of course, additional profitable properties.

In the following we discuss a primary thermometer

<sup>a)</sup>Electronic mail: cool@nanoway.fi

based on Coulomb blockade of electron tunneling and find out to what extent it meets the requirements discussed above. Further, in Sec. IV we discuss the interfacing of the sensor to two alternate signal conditioning units. All the measurements on Coulomb blockade thermometry (CBT) presented in this article, except room temperature resistance measurements, are carried out using the instruments described in Sec. IV.

### B. Principles of Coulomb blockade thermometry

CBT is based on electric conductance characteristics of tunnel junction arrays. The physical basis of CBT is thoroughly explained elsewhere<sup>6-9</sup> and only a short overview is given here.

The conductance of a tunnel junction array is determined by three energy contributions: the thermal energy  $k_B T$  at temperature  $T$ , the electric potential energy  $eV$  at bias voltage  $V$ , and the charging energy  $\epsilon_C = e^2/2C_{\text{eff}}$ , where  $C_{\text{eff}}$  is the effective capacitance of the array. In the high temperature limit where  $k_B T \gg \epsilon_C$  the dynamic conductance of a junction array can be expressed as<sup>6</sup>

$$G/G_T = 1 - (\epsilon_C/k_B T)g(eV/Nk_B T), \quad (1)$$

where  $G_T$  is the asymptotic conductance at high bias voltage and  $N$  is the number of junctions in series. The function  $g$ , which is nearly Gaussian shaped, is defined by<sup>6</sup>

$$g(x) = [x \sinh(x) - 4 \sinh^2(x/2)]/[8 \sinh^4(x/2)]. \quad (2)$$

The parameter  $V_{1/2} = 5.439Nk_B T/e$ , the full width at half minimum of the conductance dip described by Eq. (1), provides the primary thermometric quantity. There is a direct proportionality to  $T$  in  $V_{1/2}$  via the constants of nature,  $e$  and  $k_B$ ,  $N$ , and the numerical factor 5.439... originating from the shape of the function of Eq. (2). Thus, one has to know just the number of junctions in the array to extract the absolute temperature from the measured  $V_{1/2}$ . Equation (1) is strictly valid only when  $\epsilon_C/k_B T \rightarrow 0$ . A small linear correction must be applied to the measured  $V_{1/2}$  due to the nonzero depth of the dip. This correction has been calculated analytically.<sup>9</sup>

One can define another temperature dependent parameter, the depth of the dip,  $\Delta G/G_T = \epsilon_C/6k_B T$ , in Eq. (1). After calibration at some temperature  $T$  extracted from  $V_{1/2}$  this can be used as a secondary thermometer. Charging energy  $\epsilon_C$  depends on the capacitance of the junctions and it is not known precisely before measurements, but its magnitude, and this way the temperature range of operation, can be tailored by fabrication.

### C. Basic features

Figure 1 shows a typical measured differential conductance versus bias voltage of a CBT sensor. In fact, the measured quantity is resistance, but it is inverted to yield conductance. The theoretical curve of Eq. (1) is hardly distinguishable from the measured data. The thermometric parameters  $V_{1/2}$  and  $\Delta G/G_T$  are, in practice, determined by polynomial fits to selected regions.<sup>10</sup> This is significantly faster than fitting the whole theoretical curve of Eq. (1).

CBT can be operated in two modes. In the primary, or absolute, mode one measures the whole curve of Fig. 1 to get

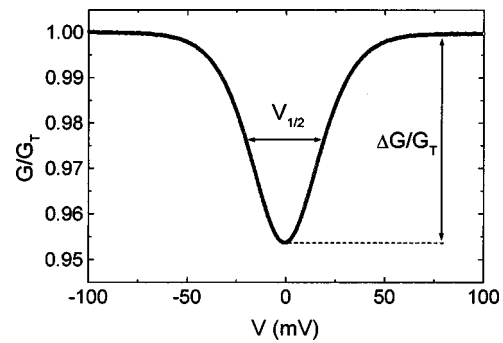


FIG. 1. Measured differential conductance of a CBT sensor with  $N=20$  at  $T \approx 4.2$  K. Both the thermometric parameters, the full width at half minimum,  $V_{1/2} \propto T$ , and the depth of the minimum,  $\Delta G/G_T \propto T^{-1}$ , are illustrated. The theoretical curve of Eq. (1) is shown as a solid line but it is hardly distinguishable from the measured data.

$V_{1/2}$ . The secondary, or relative, mode is a zero-bias measurement in which the parameter  $\Delta G/G_T$ , calibrated by a primary temperature value, is measured. The primary measurement takes typically 1–2 min whereas the zero-bias conductance can be measured much faster. The speed of the measurement is discussed in Sec. IV E.

The dependence of the depth of the minimum,  $\Delta G/G_T$ , on the capacitance of the junctions,  $C_{\text{eff}}$ , allows one to set the mean temperature of the sensor by fabricating junctions of desired overlap area. The junction capacitance can be approximated as that of a parallel plate capacitor whose area is roughly the overlap area of the electrodes separated by a thin oxide layer.

The material of our CBT sensors is aluminum. At temperatures below about 1.3 K its superconductivity must be suppressed by applying a sufficient magnetic field. The required magnitude is 0.05–0.2 T depending on the direction of the field and the thickness of the Al film.<sup>11</sup> Superconductivity can be suppressed by inserting the sensor inside a coil or by employing a permanent magnet.

Temperature range of the CBT extends from about 20 mK to 30 K and it is covered by two sensors with different mean temperatures. The depth of the conductance minimum,  $\Delta G/G_T$ , varies typically between 0.5% and 30% from the maximum to the minimum temperature of each sensor.

## II. SENSOR FABRICATION

CBT sensors are fabricated on either nitridized or oxidized silicon substrate by electron beam lithography. The standard two layer electron beam resist of poly(methylmethacrylate) (PMMA) and PMMA/MAA copolymer is used to allow two angle evaporation of aluminum. The tunnel barrier is formed by oxidizing the first Al layer at room temperature between the evaporations.

The overlap area of the tunnel junctions is about  $0.03 \mu\text{m}^2$  for the medium temperature sensor (CBT-MT,  $1 \text{ K} < T < 30 \text{ K}$ ) and about  $1.8 \mu\text{m}^2$  for the low temperature sensor (CBT-LT,  $20 \text{ mK} < T < 1.5 \text{ K}$ ). The Al film thickness is about 30 and 100 nm, respectively, for each type of a sensor. Figure 2 shows optical microscope images of the CBT arrays of each type.

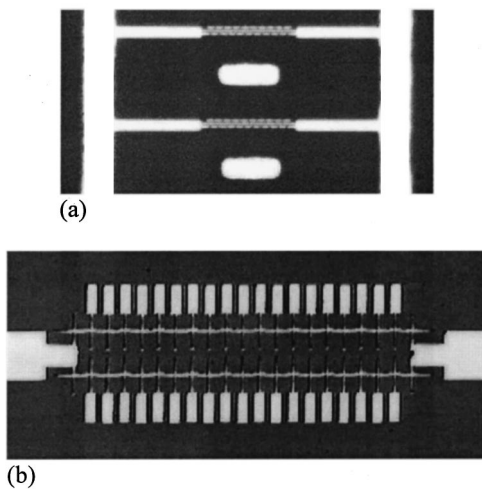


FIG. 2. Optical microscope images of CBT sensors. (a) Two of the five parallel arrays of 20 junctions of a CBT-MT for temperatures  $1\text{ K} < T < 30\text{ K}$ . The length of the arrays is  $13\ \mu\text{m}$  (b) Two parallel arrays of a sensor of LT-type for temperatures  $20\text{ mK} < T < 1.5\text{ K}$  with 20 junctions in series. The length of the arrays is  $160\ \mu\text{m}$ .

The result in Eq. (1) has been calculated for arrays with zero impedance at the ends. In the case of short arrays the impedance of the environment should be taken into account, but for long arrays, 20 junctions or more, this effect becomes negligible and does not impair the accuracy.<sup>7,9,12,13</sup> To make sure of this, the end impedance has been minimized by making the lines between the outermost junctions and the broader connecting leads as short as possible [see Fig. 2(a)].

Unfortunately, the electron dose to expose the broad lines induces the electron scatter in its immediate surroundings. This proximity effect is negligible in case of the large junctions in Fig. 2(b), but it broadens the lines close to the ends in the CBT-MT type sensors. The array is made more uniform by adding extra broad lines between the arrays. Variations in the junction area make the half width,  $V_{1/2}$ , of the sensor too small.<sup>7,9</sup> Fortunately the sensor is fairly insensitive to the fabrication errors: standard deviation of 10% in the junction area yields an error of 0.2% in  $V_{1/2}$ .

### III. CHARACTERISTICS OF THE CBT SENSORS

#### A. Accuracy and stability

The absolute accuracy of the CBT sensors is typically tested in liquid  $^4\text{He}$  bath at  $T \approx 4.2\text{ K}$  against temperature obtained from the vapor pressure of  $^4\text{He}$ , which is measured using a calibrated capacitive pressure gauge. At present the absolute accuracy is typically better than  $\pm 0.5\%$ . A histogram in Fig. 3 gives an idea of the yield and accuracy of the sensors fabricated in a way described above. A batch of 80 sensors was measured right after the fabrication process at about 4.2 K. The scatter is mostly due to the inhomogeneities in the tunnel junction arrays, and it can be reduced by more uniform electron beam exposure. No principal reasons for worse accuracy down to 0.1 K or below exist.

A common problem with aluminum based tunnel junctions is the slow drift of their resistance in air at room temperature. A resistance change in itself should not affect the

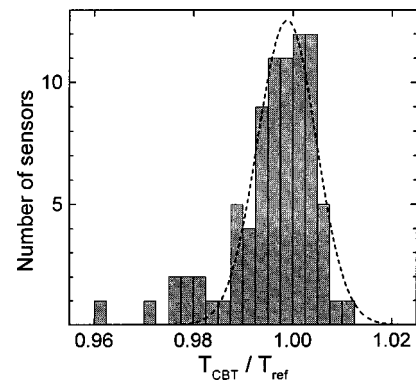


FIG. 3. Histogram of the absolute accuracy of a batch of 80 sensors measured at about 4.2 K right after fabrication. The reference temperature  $T_{\text{ref}}$  was determined by measuring the vapor pressure of liquid  $^4\text{He}$  in which the sensors were immersed. The Gaussian fit gives a mean value of the accuracy  $T_{\text{CBT}}/T_{\text{ref}} = 0.9988$  and a standard deviation  $\sigma = 0.0059$ .

properties of CBT in thermometry, but in practice this indicates that the scatter in junction parameters increases, as well, and thus the absolute accuracy is degraded. The effect of this aging on the accuracy is shown in Fig. 4. The  $V_{1/2}$  of ten sensors was measured at a temperature of about 4.2 K for several resistance values  $R$  which correspond to different measurements along the aging history of a sensor.  $R_0$  is the initial value of the sensor resistance. The accuracy versus resistance does not obey any general law, but on the average  $V_{1/2}$  decreases with increasing resistance. Fortunately the dependence is fairly weak; a relative change of less than 10% in sensor resistance should yield an absolute accuracy change of less than 0.5%.

We have not been able to reliably control the stability of the sensors by changing parameters in the fabrication process. However, stabilization is possible by not exposing the sensors to air. Hermetic sealing in an atmosphere of an inert gas, e.g., helium or even nitrogen, gives significant improvement, but the purity of the gas has proven to be very critical. Also, naturally, cooling the sensors to cryogenic temperatures stops the aging. Best results at room temperature were achieved by placing the sensor chips in vacuum. The aging can be stopped almost completely in a vacuum which is better than about 0.5 mbar. As shown in Fig. 5 the evolution of the resistance in time varies remarkably from one sensor to

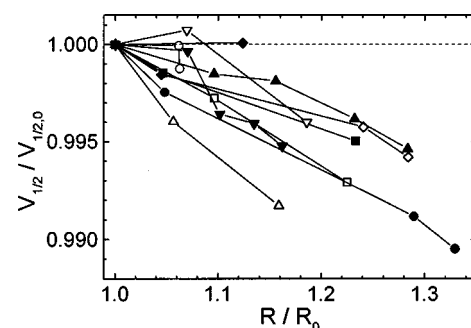


FIG. 4. Effect of aging, i.e., increase of the resistance due to the corroding effect of the surrounding atmosphere, on the absolute accuracy of the CBT measured for ten sensors at  $T \approx 4.2\text{ K}$ . The curves are normalized to start from one. Between each of the measurements the samples were let to age at room temperature in air.

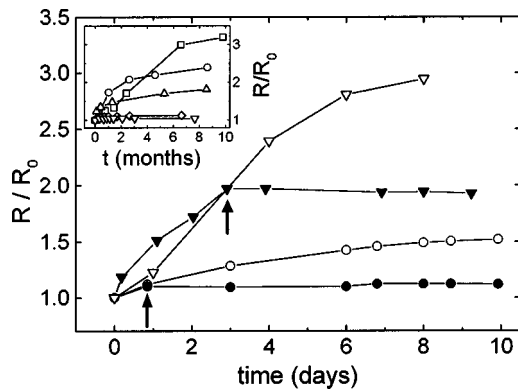


FIG. 5. Effect of vacuum on aging of the CBT sensors. Resistances are measured at room temperature. Filled symbols correspond to the sensors placed into a vacuum chamber ( $p \approx 10^{-2}$  mbar) at a moment indicated by the vertical arrows, whereas the reference sensors were stored in air (corresponding open symbols). The inset shows typical aging curves over longer time periods for unpacked sensors stored in air at room temperature.

another, actually from one fabrication batch to another, but a sufficient vacuum seems to stop even a very rapid growth of resistance. A practical vacuum encapsulation for the sensors is being developed, still ensuring thermal contact at low temperature via the proper mounting of the sensor.

## B. Temperature range and thermalization of the CBT sensor

At the high temperature end the use of CBT is presently limited by the properties of the insulating  $\text{AlO}_x$  layer of the junctions.<sup>9</sup> At bias voltages above about 20 mV per junction the conductance is voltage dependent due to the noninfinite height of the tunnel barrier. Also, the charging peak becomes lower and therefore the signal-to-noise ratio gets worse toward higher temperatures unless one makes substantially smaller junctions. This means, in practice, that temperatures above 30 K cannot be measured reliably by sensors made using the regular shadow mask evaporation techniques with aluminum.

The temperature that is measured by the CBT is that of conduction electrons which is supposed to be equal to lattice temperature. At low temperatures, however, the electron-phonon coupling in the electrodes becomes weak.<sup>8</sup> Power dissipation due to the bias voltage in the absolute measurement raises the electronic temperature above the lattice temperature. This cross-over temperature can be lowered by optimizing the geometry of the junction array. Additional cooling fins were attached to the islands between the junctions to improve the thermalization of electrons [Figs. 2(b) and 6]. By efficient thermal anchoring, electrical filtering, and shielding of the wiring we were able to measure temperatures down to 20 mK with an error of  $\leq 5\%$ .<sup>14</sup> To achieve even lower temperatures requires more efficient thermalization of the electron system by still increasing the size of the electrodes. In the relative, zero-bias measurement, heating due to the excitation voltage is always negligible.

The sensor chip does not require strain free mounting unlike many other thermometers and thus it can be fixed (e.g., glued) on almost any kind of a substrate. This way the

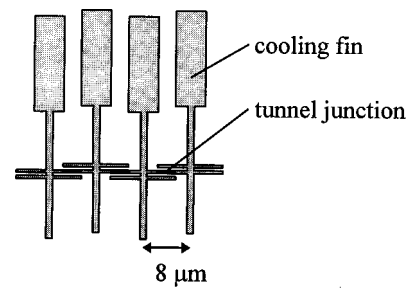


FIG. 6. Layout of the CBT sensor for low temperatures (CBT-LT). Extra cooling fins were attached to the electrodes to improve the thermalization of electrons.

thermal contact to the object, temperature of which is to be measured, can be made sufficient.

The temperature range of a single CBT sensor extends over about two decades. The whole usable temperature range can be covered by two sensors. CBT-MT for  $1 \text{ K} < T < 30 \text{ K}$  has five 20-junction arrays connected in parallel. The layout of the CBT-LT for  $20 \text{ mK} < T < 1.5 \text{ K}$  has not yet been finalized but presently we plan to have parallel chains of 40 junctions. The number of junctions in series will be increased to have a broader resistance peak at the lowest temperatures. The temperature ranges are chosen so that one can operate with  $^4\text{He}$  cooling systems using only one of the sensor types.

## C. Tolerance to magnetic field

Magnetic fields are very often present in cryogenic experiments and applications. Most of the cryogenic thermometers used so far are disturbed by the application of a magnetic field. The performance of the CBT sensors in strong magnetic fields has been tested at the Grenoble High Magnetic Field Laboratory.<sup>11</sup> A field up to 23 T was produced using a resistive magnet. The measurements were carried out at temperatures between 0.4 and 4.2 K in a single cycle  $^3\text{He}$  evaporation cryostat. A calibrated ruthenium oxide resistor was used for cross checking the temperature measurement. The magnetic field independent reading of  $^3\text{He}$  and  $^4\text{He}$  vapor pressure provided information on the stability of temperature.

Figure 7 shows the differential resistance curves measured at twelve magnetic fields up to 23 T at  $T = 1.46 \text{ K}$ . No sign of magnetic field dependence can be seen. This result

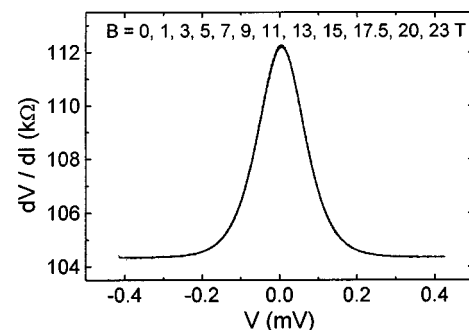


FIG. 7. Primary thermometer signal, the differential resistance  $dV/dI$ , measured at 12 different magnetic fields oriented parallel to the aluminum films in the sensor at  $T = 1.46 \text{ K}$ .

also agrees with theoretical arguments of CBT thermometry assuming that the conductance changes are primarily determined by the energetics of static charges. The absolute mode of CBT was measured at several constant magnetic fields and temperatures whereas the relative mode was tested by sweeping the field from 0 to 23 T at several constant temperatures. There was no observable effect of the magnetic field either on  $V_{1/2}$  or on  $\Delta G/G_T$  to within our accuracy of about 1%. Electrical noise, vibrations, and eddy current heating increased above 15 T and degraded the measurement accuracy. The conclusion was that CBT provides the very first magnetic field independent cryogenic primary thermometer for everyday use in laboratories. Measurements in high fields down to 20 mK are still to be performed.

#### D. Tolerance to radiation

In some applications, as in accelerators with superconducting magnets like the large hadron collider (LHC) being constructed in CERN, or in the space environment, low temperature thermometers are exposed to intense radiation. CBT sensors have been tested against neutron irradiation at the SARA cyclotron located in Grenoble, France. The sensors were irradiated by 5–10 MeV neutrons produced by stopping a 20.2 MeV deuteron beam in a 3-mm-thick beryllium target.<sup>15</sup>

In the first experiment the irradiation was done at a temperature of 4.2 K. The reference temperature was obtained from the vapor pressure of liquid  $^4\text{He}$  in small cans immersed in LHe bath close to the sensors. The total neutron fluence during about 3 days was  $1.6 \times 10^{15} \text{ cm}^{-2}$ . Such neutron fluences,  $10^{13}$ – $10^{14} \text{ cm}^{-2}$  per year, are expected in the future ATLAS experiment on the LHC accelerator in ten years.<sup>15</sup>

A change in the absolute accuracy of the sensors was observed. The change was quite linear in neutron fluence and it varied from 2% to 7% from one sensor to another at the full dose. The behavior of the sensor resistances was fairly similar to this. The lithographic layout and the fabrication process were the same for all of the six tested sensors. The substrate material was oxidized silicon.

We have not found any definite reason for the difference in the radiation tolerance between the sensors. We found no correlation between the oxide thickness of the substrate and the irradiation tolerance. The sensors had recovered in a few days almost perfectly after warming up to room temperature.

The second experiment was carried out at  $T = 1.8 \text{ K}$ . The irradiation was done in two periods. After getting a neutron fluence of  $1.4 \times 10^{15} \text{ cm}^{-2}$  the sensors were annealed up to 250 K in 4 h and immediately cooled down back to 1.8 K. The irradiation was then repeated. We used three different types of substrates as follows: samples 1 and 2, pure Si; samples 3 and 4, free-standing SiN membrane (0.4 mm  $\times$  0.4 mm  $\times$  250 nm) etched on nitridized Si; sample 5, nitridized Si. All the five sensors had almost an identical geometry. In samples 3, 4, and 5 the contact pads were, however, made longer to take the indium–solder contacts far away from the active area of the sensor. Samples 1 and 2 were on the same chip, similarly samples 3 and 4.

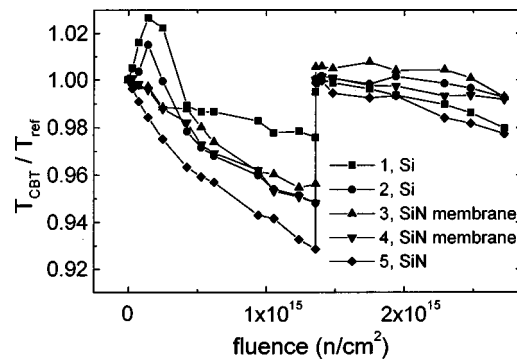


FIG. 8. Performance of CBT sensors in neutron radiation at  $T = 1.8 \text{ K}$ . Temperature obtained from the half width of the resistance peak is divided by the reference temperature. The curves are normalized to start from one. The recovery at  $1.4 \times 10^{15} \text{ cm}^{-2}$  is due to an annealing cycle.

Three parameters of the sensors were measured: the full width at half minimum of the conductance curve, the depth of the minimum, and the asymptotic resistance at high bias voltage. The reference temperature was obtained by the same method as in the first experiment.

Dependence on neutron fluence was observed in all three parameters. After the first irradiation the changes in  $V_{1/2}$  were again 2%–7% (Fig. 8). The corresponding changes in  $\Delta G/G_T$  were 5%–17%, and 5%–12% in  $G_T^{-1}$ . All the sensors recovered almost perfectly during the 4 h annealing. Within the second irradiation the changes in all the three parameters were remarkably smaller: 1%–2% in the half width, 2%–5% in the depth of the minimum, and 1%–3% in the asymptotic resistance.

One more experiment was carried out about half a year after the second test to find out if the hardening is permanent. Some of the sensors were reirradiated together with new similar sensors in the same conditions as before. In general, the changes were smaller than in the previous experiments, but the hardening proved to be short termed. The changes were actually larger in the sensors irradiated before than in the new ones.

The effect of the intensity of the neutron beam was also tested. The asymptotic resistance of one sensor was monitored during irradiation with two different beam intensities. Asymptotic resistance was chosen as the indicator because this is not sensitive to small changes in the helium bath temperature. The result was that it is the total fluence, not the intensity, that determines the radiation damage of the sensor.

The fluence used in these tests corresponds to the estimated ten year dose in the LHC accelerator. In that respect the neutron radiation hardness of the CBT sensors is not adequate, but for example the fluence required by European Space Agency for the tests of components for space applications is  $10^{10} \text{ cm}^{-2}$ .<sup>16</sup> This number is for protons, but being five orders of magnitude lower than the fluence in our tests it should not have an observable effect on the CBT sensors. Therefore, the radiation tolerance should not limit the use of CBT thermometry in space applications.

The differences between the behavior of the sensors under irradiation are somewhat unexpected and the radiation hardness seems not to be easily enhanced. Possibly the varia-

tion can be explained by nonuniformity in the properties of the oxide layer in the tunnel junctions.

## IV. CBT ELECTRONICS

### A. Measurement principle

The theoretical results on the transport properties in the CBT arrays have been calculated for conductance, but in practice it is more straightforward to measure its inverse, the resistance. The task of the electronics is to measure the differential resistance of the sensor,  $dV/dI$ , as a function of bias voltage. Such a curve is obtained in the following way. A suitable sweep voltage is applied across the sensor. A small alternating current (ac) excitation voltage is added to the bias and the ratio of the resulting ac voltage drop to the excitation current is measured. Use of low noise ac techniques is necessary to attain reasonable signal-to-noise ratio. Measurement of the ac signal is based on lock-in techniques, and this way the low frequency noise, in particular, can be suppressed.

### B. Requirements

The accuracy of the electronics should be better than  $\pm 0.1\%$  for the measured half width in order to get the maximum use of the CBT sensor. Presently the overall measurement accuracy is limited by reproducibility in fabrication and consistency of the sensors to about  $\pm 0.5\%$ .

The amplitude of the ac excitation must be kept much smaller than the half width of the resistance peak. An excessive ac amplitude will round the peak and result in too large a half width. In practice, the amplitude has to be less than about 5% of  $V_{1/2}$ . At the lower end of the temperature range, 20 mK, the half width is only about 0.4 mV for a sensor with  $N=40$ . Thus, the excitation voltage has to be less than 20  $\mu\text{V}$ . This sets high requirements for the quality of the electronics. One can naturally correct for the effect of a large excitation level, if its use is necessary. At temperatures above 1 K the requirements are not that severe.

The bias voltage range must be at least about 2.5 times  $V_{1/2}$  on both sides of zero to get a reliable value for the asymptotic resistance  $G_T^{-1}$ . On the other hand, the range must not be too large in order to be able to zoom into the interesting region of the resistance peak.

The effect of noise on the accuracy of determining  $V_{1/2}$  has been studied as well.<sup>10</sup> Gaussian noise with a standard deviation  $\sigma$  was added to the theoretical curve  $g$  of Eq. (2). In order to obtain an accuracy of  $\pm 0.1\%$  in measuring  $V_{1/2}$  the ratio of  $\sigma$  to the depth of the conductance minimum,  $\Delta G/G_T$ , must not exceed 0.004 according to the computer simulations. For peaks with  $\Delta G/G_T$  of several percent this requirement is straightforward to attain. For example, if  $\Delta G/G_T = 3\%$  we need  $\sigma \approx 10^{-4}$  which is still easy to obtain. At the upper end of the temperature range, 30 K,  $\Delta G/G_T$  is typically less than 0.5%. To obtain an accuracy of  $\pm 0.1\%$ , the noise level in the measured signal should be  $\sigma \leq 2 \times 10^{-5}$ . This is already hard to reach in practice even if the

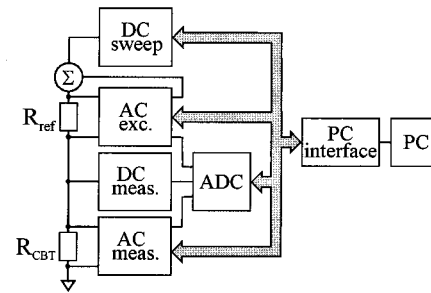


FIG. 9. Block diagram of the DVS-10. The analog part of the instrument consists of a sweep unit, an ac excitation circuit (reference channel), a bias measurement circuit, and an ac measurement circuit (signal channel).

excitation amplitude can be increased as the resistance peak broadens toward higher temperatures; in a noisy environment it may be impossible.

The requirements mentioned above mean that the instrument must have several selectable excitation amplitudes and ranges of bias voltage. The resolution of the analog-to-digital conversion has to be close to  $10^{-5}$ , which equals 16 bits. Particular attention must be paid to the measurement of the direct current (dc) bias voltage across the sensor. The accuracy in the half width,  $V_{1/2}$  of the resistance peak, and thereby in the absolute temperature cannot be better than the absolute accuracy of the bias voltage measurement.

We have developed two different prototypes of instruments for different applications. The DVS-10, operating with a PC computer, is intended to be a general-purpose instrument for measuring nonlinear resistors. The other prototype, developed in cooperation with Mitron company,<sup>17</sup> is a stand-alone instrument having an embedded processor. It is an economic and simple device developed merely for the CBT measurement.

### C. PC assisted CBT instrument

The DVS-10 is an advanced instrument based on an ac resistance bridge AVS-47<sup>18</sup> but modified in such a way to make it suitable for measuring nonlinear resistors, regardless of their resistance level or shape of the nonlinearity. The DVS-10 operates under a PC computer control and it has a multiplexed input for four sensors. A general block diagram of the instrument is shown in Fig. 9. For simplicity, the multiplexer is not shown. Together with the software developed for the CBT application it provides a versatile thermometer electronics for laboratory use. Several changes were made to the basic resistance bridge as will be described below.

#### 1. Resistance bridge circuit

Here we describe the general principle and operation of the resistance bridge circuit which is similar to that of the AVS-47. It consists of the reference channel and the signal channel shown in Fig. 9.

In the reference channel (Fig. 10) a square-wave excitation is generated from a dc reference voltage by using a chopper. This wave form, which is a couple of volts in amplitude, is attenuated to the desired level and fed to a preamplifier via a summing stage. Inputs of the preamplifier are connected to a reference resistor  $R_{\text{ref}}$ . The output of the pre-

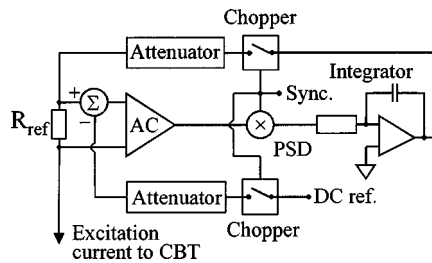


FIG. 10. Reference channel of the resistance bridge circuit of the DVS-10.

amplifier is zero if the two inputs are equal. If the voltage drop across  $R_{\text{ref}}$  due to the excitation current is not equal to the reference signal, the output of the preamplifier will not be zero. This output is rectified by a phase sensitive detector (PSD) at the excitation frequency, and then integrated. The integrator output is chopped and attenuated to form the excitation voltage, which is fed to the reference resistor. (In fact, it is first added to the dc sweep as depicted in Fig. 9.) As long as the preamplifier inputs are different, the integrator output changes, until the loop is in balance and the excitation current is  $I = V_{\text{ref}}/R_{\text{ref}}$ .

A similar loop in the signal channel (Fig. 11) measures the voltage drop across the CBT sensor, which is  $V_{\text{CBT}} = IR_{\text{CBT}} = V_{\text{ref}}R_{\text{CBT}}/R_{\text{ref}}$ . The output of the signal channel integrator is filtered in order to suppress the effect of the ac signal. This is done because of the sampling nature of the analog-to-digital (A/D) converter.

All the three attenuators in the reference and signal channels have identical steps in 1:3 sequence so that the two feedback signals are attenuated by the same factor as the dc reference voltage on each of the seven selectable excitation levels. The reduction of the overall loop gain, when the attenuation is increased, is compensated by an equivalent increase of the amplifier gains.

The bias voltage is attenuated from a large voltage swing of a ramp generator. Nevertheless, it can introduce additional noise to the total excitation current. From this noise, the phase sensitive detection in the reference channel would pick the component that is at, or very close to, the excitation frequency  $f$ . Fortunately, the operation principle of the instrument automatically suppresses this additional noise. The phase sensitive detector, the integrator, and the attenuator together with the preamplifier make up a servo loop that maintains the correct value of the ac excitation across  $R_{\text{ref}}$ . Frequencies far from  $f$  cannot be compensated, but they do not impair the performance, either.

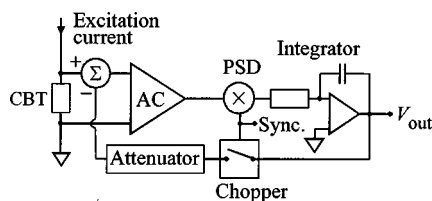


FIG. 11. Signal channel of the resistance bridge circuit of the DVS-10. The output is  $V_{\text{out}} \propto (dV/dI)_{\text{CBT}}$ .

## 2. Sweep unit

The dc voltage sweep in DVS-10 is a simple analog ramp generator having comparators for negative and positive limits of equal magnitude. A start pulse releases the reset and the output starts to rise from the negative limit at the selected rate toward the positive limit.

The idea is to work with a high sweep amplitude at variable sweep times, and to attenuate this amplitude so that the desired sweep ranges are obtained. The noise from a resistive attenuator is lower than the noise from a ramp generator. This keeps the signal-to-noise ratio of the sweep unit sufficiently low even in very narrow sweeps at low temperatures. Seven selectable sweep times between 30 and 360 s, and ten different voltage ranges are available.

## 3. Modification of the amplifiers

The lowest nominal excitation of the DVS-10 is  $10 \mu\text{V}$  and therefore the gain of the amplifiers has to be high. One of the problems is to prevent the saturation of amplifiers in the presence of a dc voltage sweep. The dc decoupling is realized by using capacitors in the inputs of the preamplifiers. This is done in such a way that the discharge paths of the capacitors do not impair the linearity of the bridge. In the presence of a dc sweep, the first decoupling stage will output a constant voltage (differentiated linear ramp). This voltage could still saturate the amplifier. Another decoupling stage (differentiated constant voltage) had to be inserted to avoid this. Although the phase sensitive detectors are insensitive to a dc voltage input, such a voltage would result in a sawtooth component in the integrator output, which would then require filtering.

## 4. Measuring the dc bias across the sensor

In a resistance bridge, an ac excitation current cannot be directly added to a dc bias voltage because it would be suppressed by the low impedance of the voltage source. Therefore, the summing must be done at a higher impedance level. The voltage across the sensor is a sum of dc and ac voltages. The ac component must be eliminated from the signal while measuring the dc bias. We developed a way to subtract the ac component quickly by making use of the feedback signals. This method is faster than filtering and it reduces the ac component by a factor of 100 which is satisfactory for the present application.

## 5. Analog-to-digital converter

The A/D converter suitable for this application should be sampling and have a resolution preferably more than 16 bits. Such an ADC is rather expensive and therefore we designed one ourselves. The ADC is based on a sampling capacitor, which is discharged by a constant current until a comparator voltage, which stays at a constant value, is achieved. The sampling capacitor is successively connected to zero, to a calibration voltage and to an unknown voltage. These three readings are used to calculate the ADC offset, the scale factor, and the unknown voltage. The standard deviation of the conversion is equal to 18 bits and the speed is about three conversions per second. In the case of an absolute measure-

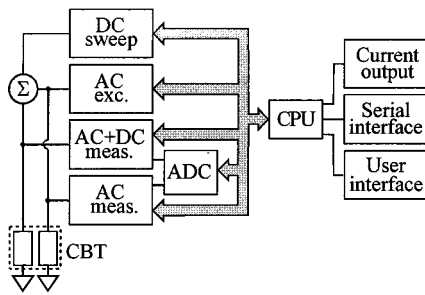


FIG. 12. Block diagram of the stand-alone CBT instrument. The ac+dc channel is for the absolute measurement mode and the ac channel is for the relative mode. Only one of the sensor pairs is shown for simplicity.

ment (sweep) the two calibrations are performed only once in the beginning to make the ADC faster. The computer driving the instrument must be almost entirely devoted to this A/D converter during the measurement.

**6. Operation**

A software for Windows 95 and NT was made to operate the DVS-10 with CBT sensors.<sup>19</sup> In the first version the instrument is used manually, that is, the measurement parameters, sweep time and range, and excitation amplitude are chosen by the user. An automated version is being developed.

One can operate one to four sensors in an absolute or in a relative temperature measurement mode. In the absolute mode the sweep is done either once or repeatedly for the chosen sensors. Normally a suitable sweep time is 2 min which thus gives the rate at which temperature is being read. In order to get more frequent temperature information, about one reading per second, one can monitor the zero-bias resistance which is calibrated by the absolute measurement. In this relative mode one can choose the time interval between successive calibrations.

The measured resistance curves are analyzed<sup>10</sup> automatically giving the absolute temperature and the calibration factor for the relative mode. The temperature versus time for each sensor as well as the  $dV/dI$  versus bias voltage curve are shown in graphics windows of the program.

**D. Stand-alone CBT instrument**

The other prototype developed for CBT measurements is a stand-alone instrument that does not require a separate PC computer to operate. An embedded processor is used to control the temperature measurement. The temperature readings are available in terms of a four-digit display, an analog current output, and an RS232 port. The instrument can be controlled also by a PC via the serial port. The absolute value of the sensor resistance is not measured which enables the use of a more simple circuit than that of the DVS-10. The basic principle of the measurement, based on ac excitation and lock-in techniques is, however, the same in both the devices.

The instrument makes use of the two operation modes of the CBT so that one can have semicontinuous relative measurement even during the sweep. The plan is to operate two double sensors. These two sensors can be of either of the two

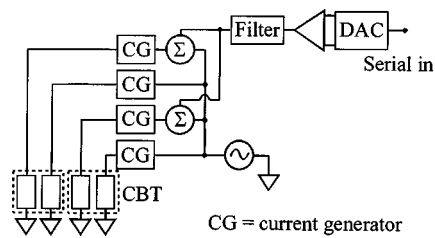


FIG. 13. Excitation and sweep unit of the stand-alone CBT instrument.

CBT types, both having one set of junction arrays for the primary measurement and another similar one for the secondary measurement.

The construction of the instrument is depicted in Fig. 12 as a block diagram. For simplicity only one pair of sensors is illustrated. Operation of the main parts of the circuit is described below.

**1. ac excitation and dc sweep**

Generation of the measurement current consisting of a linear dc sweep and a small ac excitation is shown in Fig. 13. It is realized by using voltage controlled buffered Howland-type current generators.<sup>20</sup> Four generators are needed: an ac+dc generator for the absolute temperature measurement and an ac generator for the relative measurement for both the two double sensors. The sinusoidal ac signal is produced by a commercial precision wave form generator at a frequency of about 22 Hz. A serially controlled 14-bit digital/analog (D/A) converter generates the voltage sweep from which high frequency noise due to the voltage steps is suppressed by a low-pass filter. The ac excitation and the bias sweep are combined by an inverting summing amplifier (symbol ‘Σ’ in Fig. 13). The ac amplitude and the sweep range are proportional to each other (ratio 1:165), and their magnitude is set by switching between four different input resistors (not shown in Fig. 13).

**2. ac and dc channels**

The two measurement channels of Fig. 12 are multiplexed for measuring either of the sensor pairs: the ac+dc channel for the absolute measurement mode and the ac channel for the relative mode. The structure of the ac+dc channel is shown in Fig. 14. The ac channel is similar to this except for the missing ‘bias out’ branch. In the ac measurement the voltage across the CBT sensor is filtered and amplified before feeding it to a PSD. The reference signal is taken from the oscillator (Fig. 13) and it is phase shifted. A high-pass filter eliminates the dc voltage and a notch filter was added to reject the noise from the mains voltage. The ac component is

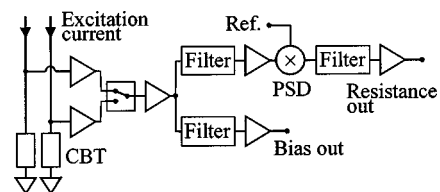


FIG. 14. ac+dc channel of the stand-alone CBT instrument multiplexed for measuring either of the two sensors in absolute mode.

removed from the signal in the dc measurement by a low-pass filter and the filtered signal is amplified by a programmable dc amplifier. A commercial 16-bit ADC was chosen for the A/D conversion of the two output voltages.

### 3. Operation

The instrument has three operation modes: two manual modes in which the user chooses the sensor and the measurement range, and an automatic mode. In the absolute mode, the sweep that takes about 2 min is continuously repeated for the chosen sensor. Thus, one gets one absolute temperature reading per 2 min.

In the relative mode, continuous zero-bias measurement yielding about three readings per second is performed. These readings are converted into temperature via the calibration in the absolute mode. After this, the relative measurement is continued and recalibrations are performed at the request of the user. During the calibration sweep the rate of the temperature readings from the relative measurement is about one per second.

In the third mode the parameters are chosen automatically and the relative measurement is run with automatic calibration by the absolute measurement. The calibration is performed after switching on the instrument and then in a suitable sequence. The measured curves are analyzed similarly as in the CBT software of the DVS-10.

### E. Performance

The performance of the CBT electronics has been tested. The noise level with different measurement settings and the step response of the measuring circuit was determined for the PC assisted CBT instrument. The speed and the noise in absolute mode were measured also for the stand-alone instrument. Other tests are still to be performed.

Noise level in the relative mode was determined by measuring the zero-bias resistance,  $R_0$ , of a CBT-MT-type sensor at 4.2 K with five different excitation voltages (Fig. 15). The relative standard deviation values,  $\sigma/R_0$ , were converted into scatter in temperature by dividing the absolute values of  $\sigma$  by the height of the resistance peak, which in this case was about 3% of the asymptotic resistance. To eliminate possible noise of the sensor itself, a metal film resistor at 4.2 K with same resistance value as the CBT (110 k $\Omega$ ) was measured with the same settings: The results overlapped with those obtained with the CBT sensor.

The reproducibility in the results of the absolute mode was tested by measuring ten resistance curves of the same sensor at 4.2 K with each of the four different excitation voltages of the DVS-10. The data are presented in Fig. 15. Only one data point is obtained with the stand-alone instrument because the excitation amplitude cannot be set separately. The proper excitation amplitude in the absolute mode at 4.2 K is 1–2 mV, which therefore yields a root mean square (rms) scatter of about  $10^{-3}$  in temperature. In the relative measurement a slightly larger excitation can be used, such that in practice the rms scatter in temperature is about  $10^{-3}$  in that mode, as well.

The noise level in Fig. 16 was measured with a cooled resistor with (absolute mode) and without (relative mode)

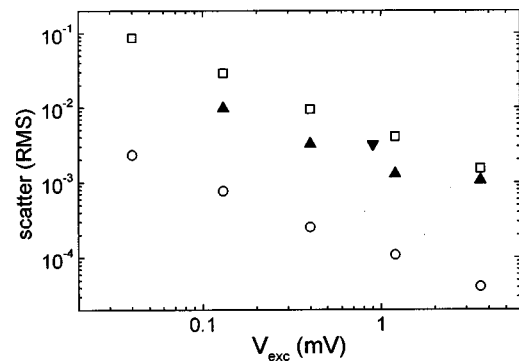


FIG. 15. Standard deviations of CBT measurements with different excitation voltages measured at about 4.2 K. At this temperature  $\Delta G/G_T \approx 3\%$  for this sensor, and  $R_T = G_T^{-1} \approx 110$  k $\Omega$ . Open circles are from the relative mode where the standard deviation of 100 data points of zero-bias resistance is divided by their mean value. Open squares are from the same measurement but converted into scatter in temperature. Up triangles show the reproducibility of the absolute mode when ten successive sweeps were made. The down triangle is from a similar measurement made with the stand-alone instrument. All the other data points are measured by the PC assisted instrument, DVS-10. In this case the optimum excitation level is 1–2 mV for the absolute mode and few millivolts for the relative mode.

bias sweep. The excitation amplitude was 1.2 mV. The presence of a relatively large dc voltage,  $\pm 0.15$  V at maximum, does not significantly impair the performance. The standard deviation is  $5 \times 10^{-5}$  in the relative measurement and  $1 \times 10^{-4}$  in the presence of the bias voltage. This meets the requirement for the noise in conductance curve mentioned in Sec. IV B.

The speed of the measurement circuit was tested for both instruments by measuring the step response. This was done by switching a resistor at room temperature from 100 to 110 k $\Omega$  in the relative measurement mode. The result in Fig. 17 gives an idea how fast temperature changes can be followed. In case of the DVS-10 the real settling time from initial to final value is probably shorter than 1.5 s indicated in the figure, because here it is limited by the sampling rate of the AD converter. For the stand-alone instrument this settling time, about 2 s, is long compared to the output rate and for

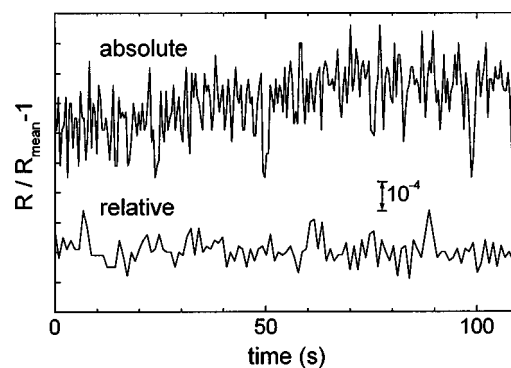


FIG. 16. Noise level of the output of the DVS-10. A standard 100 k $\Omega$  metal film resistor at 4.2 K was measured in the two modes. The bias range was  $\pm 150$  mV in the absolute mode, and the excitation amplitude was 1.2 mV in both modes. The standard deviation is  $4.6 \times 10^{-5}$  in the relative zero-bias measurement and  $1.1 \times 10^{-4}$  in presence of the bias voltage sweep in the absolute mode.

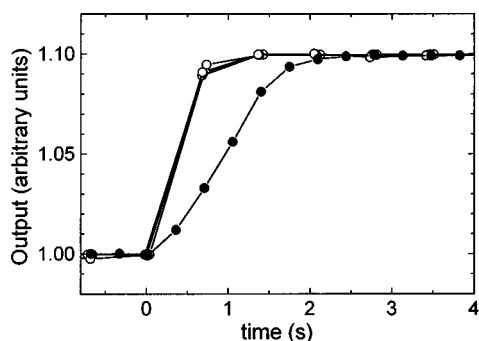


FIG. 17. Step response of the two CBT instruments. A resistor at room temperature was switched from 100 to 110 k $\Omega$  and the output was recorded. Open and solid circles correspond to the PC assisted and to the stand-alone instrument, respectively. The former was tested using four different excitation amplitudes.

this instrument it gives the rate at which it follows temperature changes.

## V. DISCUSSION

The properties of CBT have been thoroughly tested and it has been developed to a level close to a commercial product. Two signal conditioning units for CBT measurements have been developed and tested, first of which has been used intensively in testing the sensors. The requirements for the electronics can be reached as we have shown in the prototype tests. Both prototypes have a short-term reproducibility of 0.3% or better for the absolute temperature.

We have shown that CBT sensors can be produced with a reasonably high yield. The performance of CBT has been found excellent in a high magnetic field. We propose CBT as the first magnetic field independent primary thermometer for an everyday laboratory use.

## ACKNOWLEDGMENTS

This work has been supported by TEKES, Technology Development Centre of Finland and Jyväskylä Science Park. The authors thank Eero Sarkki, Jussi Toppari, Kari Hirvi, and Kimmo Kinnunen for their contributions, and Christoph Balle and Juan Casas-Cubillos for their useful comments. The research group from I. P. N. Orsay, led by T. Junquera, is thanked for realizing the irradiation experiments.

- <sup>1</sup>F. Pobell, *Matter and Methods at Low Temperatures*, 2nd ed. (Springer, Berlin, 1996).
- <sup>2</sup>T. J. Quinn, *Temperature* (Academic, New York, 1983).
- <sup>3</sup>L. G. Rubin, *Cryogenics* **37**, 341 (1997).
- <sup>4</sup>H. Preston-Thomas, *Metrologia* **27**, 3 (1990).
- <sup>5</sup>R. J. Soulen, Jr. and W. E. Fogle, *Phys. Today* **50**, 36 (1997).
- <sup>6</sup>J. P. Pekola, K. P. Hirvi, J. P. Kauppinen, and M. A. Paalanen, *Phys. Rev. Lett.* **73**, 2903 (1994).
- <sup>7</sup>K. P. Hirvi, J. P. Kauppinen, A. N. Korotkov, M. A. Paalanen, and J. P. Pekola, *Appl. Phys. Lett.* **67**, 2096 (1995).
- <sup>8</sup>J. P. Kauppinen and J. P. Pekola, *Phys. Rev. B* **54**, R8353 (1996).
- <sup>9</sup>Sh. Farhangfar, K. P. Hirvi, J. P. Kauppinen, J. P. Pekola, J. J. Toppari, D. V. Averin, and A. N. Korotkov, *J. Low Temp. Phys.* **108**, 191 (1997).
- <sup>10</sup>K. P. Hirvi and J. P. Pekola, *Comput. Phys. Commun.* **106**, 69 (1997).
- <sup>11</sup>J. P. Pekola, J. J. Toppari, J. P. Kauppinen, K. M. Kinnunen, A. J. Manninen, and A. G. M. Jansen, *J. Appl. Phys.* **83**, 5582 (1998).
- <sup>12</sup>Sh. Farhangfar, A. J. Manninen, and J. P. Pekola (to be published).
- <sup>13</sup>P. Joyez and J. Esteve, *Phys. Rev. B* **56**, 1848 (1997).
- <sup>14</sup>T. A. Knuuttila, K. K. Nummilla, W. Yao, J. P. Kauppinen, and J. P. Pekola, *Physica B* (in press).
- <sup>15</sup>B. Merkel, J. Collot, P. De Saintignon, G. Mahout, A. Belymam, and A. Hoummadaand, *Nucl. Instrum. Methods Phys. Res. B* **134**, 217 (1998).
- <sup>16</sup>European Space Agency, Single event effects test method and guidelines, ESA/SCC Basic Specification No. 25 100.
- <sup>17</sup>Mitron Oy, P.O. Box 113, FIN-30101 Forssa, Finland.
- <sup>18</sup>AVS-47 resistance bridge manufactured by Picowatt.
- <sup>19</sup>The software was made by Fotocomp Oy, Ylistönmäentie 31, FIN-40500 Jyväskylä, Finland.
- <sup>20</sup>W. G. Jung, *IC Op-Amp Cookbook*, 3rd ed. (SAMS, Prentice Hall, Carmel, 1994).